Original Article

Clinical usefulness of 18F-fluorodeoxyglucose positron emission tomography/computed tomography for patients with primary liver cancer with special reference to rare histological types, hepatocellular carcinoma with sarcomatous change and combined hepatocellular and cholangiocarcinoma

Hideki Ijichi,[1] Ken Shirabe,[1] Akinobu Taketomi,[1] Tomoharu Yoshizumi,[1] Toru Ikegami,[1] Youhei Mano,[1,2] Shinichi Aishima,[2] Koichiro Abe,[3] Hiroshi Honda[3] and Yoshihiko Maehara[1]

[1]Department of Surgery and Science, Kyushu University, [2]Department of Anatomic Pathology, Kyushu University, and [3]Department of Clinical Radiology, Graduate School of Medical Sciences, Kyushu University, Fukuoka, Japan

Aim: The role of 18F-fluorodeoxyglucose positron emission tomography (FDG-PET) in the diagnosis and staging of primary liver cancer has been demonstrated in several reports. However, no preoperative evaluations of sarcomatous hepatocellular carcinoma (HCC) and combined hepatocellular and cholangiocarcinoma (cHCC-CC) with FDG-PET have been reported so far.

Methods: Fifty-three HCC patients and three cHCC-CC patients who received liver resection or living-donor liver transplantation were enrolled in this study. All 56 patients had undergone preoperative FDG-PET, and a total of 67 HCC and three cHCC-CC were analyzed histologically. The relationship between clinicopathological features and the maximum standardized uptake value (SUVmax) of tumors were evaluated.

Results: The detection rate of HCC by FDG-PET was 43.3 %, and the sensitivity of FDG-PET for the detection of HCC was

significantly associated with tumor differentiation, tumor size and microvascular invasion. All three cHCC-CC were detected by FDG-PET. The SUVmax values of the three sarcomatous HCC (SUVmax 14.1, 18.6 and 25.0) and the three cHCC-CC (SUVmax 9.9, 12.0 and 13.0) were higher than that of the poorly differentiated HCC (mean SUVmax 5.7 ± 2.3).

Conclusion: SUVmax may be a useful diagnostic tool for the preoperative evaluation of the aggressiveness of primary liver cancers such as sarcomatous HCC and cHCC-CC.

Key words: 18F-fluorodeoxyglucose positron emission tomography, combined hepatocellular and cholangiocarcinoma, hepatocellular carcinoma, sarcomatous hepatocellular carcinoma

INTRODUCTION

POSITRON EMISSION TOMOGRAPHY (PET) using 18F-fluorodeoxyglucose (FDG) has become standard procedure for the detection of a variety of malignant tumors.[1] It is considered a useful diagnostic tool for tumor characterization and assessing therapy response.[2] For hepatocellular carcinoma (HCC), however, several reports suggest that the sensitivity of FDG-PET (50–55%) is insufficient.[3,4] Because the enzymatic activity of well-differentiated HCC cells is similar to that of the surrounding normal liver, the accumulation of FDG in these tumors is low, and the role of FDG-PET imaging in the early detection of HCC is limited.[5] On the other hand, previous studies have demonstrated that FDG accumulation is increased in undifferentiated HCC, and recently, preoperative FDG-PET has been shown to be closely associated with tumor differentiation and prognosis in HCC patients.[6,7]

481

The histological differentiation grade is an important prognostic factor for HCC.[8] Once cancer is established, HCC dedifferentiates to a more malignant histology in a multistep fashion, from well- and moderately to poorly differentiated tumors.[9] Although the prognosis of well-differentiated HCC is good following resection, poorly differentiated HCC have a poor prognosis due to a high rate of vascular invasion and metastasis.[10,11] The basic histological pattern of HCC is trabecular; however, a sarcomatous appearance has been sporadically reported as one of the histological features of HCC.[12] Approximately 1.8% of all resected HCC have a sarcomatous feature, usually associated with a very poor prognosis because of its rapid growth, low resectability and frequent recurrence after resection.[13,14]

Combined hepatocellular and cholangiocarcinoma (cHCC-CC) is a rare primary liver cancer that contains the histological features of both HCC and CC.[15] cHCC-CC has been reported to show frequent vascular invasion and lymph nodes metastasis, and has a poorer prognosis than HCC.[16,17] It is difficult for patients with cHCC-CC to get a correct preoperative diagnosis because of the lack of a sensitive diagnosis procedure.[18]

Although previous studies have shown that FDG-PET is useful for evaluating various liver tumors, there have been no reports regarding preoperative FDG uptake in resectable sarcomatous HCC and cHCC-CC. In the present study, we retrospectively investigated the feasibility of FDG-PET for the detection of different types of primary liver cancer including sarcomatous HCC and cHCC-CC.

METHODS

Patients

IN THIS STUDY, we retrospectively reviewed 53 HCC patients and three cHCC-CC patients who received liver resection (LR) or living-donor liver transplantation (LDLT) at Kyushu University Hospital between April 2010 and August 2011. There were 35 male and 21 female patients, and the mean age (± standard deviation [SD]) of the patients was 65 ± 12 years (range, 36–87). All 56 patients were diagnosed as having HCC or cHCC-CC by conventional radiologic imaging and FDG PET/computed tomography (CT). Thirteen patients with HCC in cirrhosis underwent LDLT, and the other 43 patients with HCC or cHCC-CC underwent LR. Among the HCC patients, 29 had a single lesion, and the other 24 had multiple lesions. Among the cHCC-CC patients,

one had a single lesion and the other two had multiple lesions.

Patient follow up

After discharge, all patients were examined for recurrence by ultrasound and by tumor markers every 1–3 months. Dynamic CT was performed every 6 months. Patients with any sign of recurrence and/or inconclusive imaging studies underwent additional FDG PET/CT. All of the patients were followed up while they were alive.

FDG PET/CT

[18]F-Fluorodeoxyglucose positron emission tomography studies were performed with Discovery ST Elite (GE Healthcare, Milwaukee, WI, USA) and Biograph mCT (Siemens AG, Erlangen, Germany) PET/CT scanners. All patients fasted for at least 4 h before FDG administration, and 185 MBq of FDG was i.v. administrated to each patient. Approximately 60 min after the FDG injection, whole-body PET images were acquired from thigh to head with 7–10 bed positions. The Discovery ST Elite scanner consists of a 16-slice multidetector CT and bismuth germanium oxide crystal. The unenhanced CT was performed first with the following parameters: 5-mm slice thickness, 120 kV, 30–250 mAs with auto mode (Smart mA). Then, PET images were obtained in 3-D mode for 3 min per bed position with a 3.27-mm slice thickness, at 70 cm field of view (FOV) in a 128×128 matrix. Based on the CT data, transmission maps were created and used for the attenuation correction of the PET images. The PET data were reconstructed using a 3-D ordered subset expectation maximization (3D-OSEM) algorithm (VUE Point Plus) with two iterations and 28 ordered subsets. A 6-mm post-filter of full-width at half maximum (FWHM) was applied. The Biograph mCT scanner is equipped with a 128-slice multidetector CT and lutetium crystal. The unenhanced CT was performed at 120 kV with automatic mAs adjustment (Care Dose 4D) and the slice thickness was 3 mm. The PET emission time was 2 min per bed position. The PET images were acquired with a 2-mm slice thickness, at 70 cm FOV in a 256×256 matrix. The concomitant CT data were used for attenuation correction. The PET data were reconstructed using a 3D-OSEM algorithm with two iterations and 21 subsets. Time of flight and point spread function techniques were also used for the image reconstruction (ultra-HD-PET). A 3-D Gaussian filter of 6-mm FWHM was applied. The PET images were qualitatively evaluated to assess whether the FDG uptake in the tumor was (PET positive status) or was not

(PET negative status) significantly higher than in the surrounding non-cancerous hepatic parenchyma.

Histopathological study

A total of 67 HCC and three cHCC-CC were evaluated histologically. Formalin-fixed specimens were embedded in paraffin. Deparaffinized 4-μm sections were stained with hematoxylin–eosin for microscopic evaluation. The histopathological definition of HCC and the criteria for cHCC-CC were based on the classification proposed by the World Health Organization. The cHCC-CC contain unequivocal hepatocellular and cholangiocellular components that are intimately admixed. The HCC displayed a trabecular pattern with little stroma, a pseudoglandular pattern with or without bile production, abundant eosinophilic cytoplasm, and immunoreactivity for Hep par 1. The CC was defined by a definite glandular pattern with fibrous stroma, low columnar cells with round vesicular nuclei, mucin production confirmed by Alcian blue, and immunoreactivity for cytokeratin 19 but not Hep par 1.

Statistical analysis

All statistical analyses were performed using the StatView ver. 5.0 software package. Continuous variables were compared using the Mann–Whitney U-test or Student's t-test. The χ^2-test was used for categorical variables. The differences were considered to be significant if $P < 0.05$.

RESULTS

Patients with HCC

PATIENT CHARACTERISTICS ARE summarized in Table 1(a). The mean age (± SD) was 66 ± 12 years (range, 36–87), and the sex ratio (M : F) was 32:21. Thirty-two patients (60.4%) were seropositive for hepatitis C virus, 11 for hepatitis B surface antigen (20.8%) and 10 (18.8%) had non-B/non-C etiologies. Twelve of the 53 patients had a serum α-fetoprotein (AFP) level of more than 100 ng/mL (median, 11.8; range, 1.6–994 600) and 24 patients had a serum des-γ-carboxy prothrombin (DCP) level above 100 mAU/mL (median, 81; range, 10–109 730). Twenty-nine patients with solitary tumors were divided into two groups: PET positive ($n = 16$) and PET negative ($n = 13$). Although there was no significant difference in serum AFP levels between the PET positive and negative groups (110.2 ± 196.9 and 132.9 ± 372.7 ng/mL, respectively), the PET positive group had higher serum

Table 1 Characteristics of patients with HCC and clinicopathological data of HCC

a. Characteristics of patients with HCC

Characteristic	No. of patients (%)
Total number of patients	53
Age (years)	
Mean (range)	66 (36–87)
Sex	
Male : female	32 (60.4):21 (39.6)
Etiology of liver disease	
Hepatitis B	11 (20.8)
Hepatitis C	32 (60.4)
Other	10 (18.8)
Child–Pugh classification	
A	40 (75.5)
B	6 (11.3)
C	7 (13.2)
Tumor stage (UICC)	
I	21 (39.6)
II	25 (47.2)
III	5 (9.4)
IV	2 (3.8)
Type of hepatic surgery	
Resection	40 (75.5)
Liver transplantation	13 (24.5)
Tumor number	
Solitary	29 (54.7)
Multiple	24 (45.3)
Preoperative serum AFP (ng/mL)	
Median (range)	11.8 (1.6–99 4600)
Preoperative serum DCP (mAU/mL)	
Median (range)	81 (10–109 730)

b. Clinicopathological data of HCC

Characteristic	No. of HCC (%)
Total number of nodules	67
Tumor differentiation	
Well	7 (10.4)
Moderately	47 (70.1)
Poorly	9 (13.4)
Undifferentiated	1 (1.5)
Moderately with sarcomatous change	1 (1.5)
Poorly with sarcomatous change	2 (3.0)
Tumor size (cm)	
Mean ± SD	3.4 ± 3.4
Microvascular invasion	16 (23.9)

AFP, α-fetoprotein; DCP, des-γ-carboxy prothrombin; HCC, hepatocellular carcinoma; SD, standard deviation; UICC, Union for International Cancer Control.

Table 2 Association between PET status and clinicopathological data of HCC

Characteristic	PET negative ($n = 38$)	PET positive ($n = 29$)	P-value
Tumor differentiation (%)			<0.05
Well	7 (100)	0 (0)	
Moderately	31 (66)	16 (34)	
Poorly	0 (0)	9 (100)	
Undifferentiated	0 (0)	1 (100)	
Moderately with sarcomatous change	0 (0)	1 (100)	
Poorly with sarcomatous change	0 (0)	2 (100)	
Tumor size (cm)			
Mean ± SD	2.1 ± 1.5	5.1 ± 4.3	<0.05
Microvascular invasion (%)	4 (11)	12 (41)	<0.05

HCC, hepatocellular carcinoma; PET, positron emission tomography; SD, standard deviation; UICC, Union for International Cancer Control.

DCP levels than the PET negative group (529.6 ± 748.3 and 54.2 ± 50.7 mAU/mL, respectively; $P < 0.05$) (± SD). Using the modified Union for International Cancer Control staging system, we enrolled 21 (39.6%) stage I patients, 25 (47.2%) stage II patients, five (9.4%) stage III patients and two (3.8%) stage IV patients.

The characteristics of HCC are summarized in Table 1(b). The histological grades were well differentiated in seven HCC (10.4%), moderately differentiated in 47 (70.1%), poorly differentiated in nine (13.4%), undifferentiated in one (1.5%), moderately differentiated with sarcomatous change in one (1.5%) and poorly differentiated with sarcomatous change in two (3.0%). Mean tumor size (± SD) was 3.4 ± 3.4 cm, and microvascular invasion was observed in 16 HCC (23.9%). The detection rate of HCC by PET was 43.3%. The sensitivity of PET for the detection of HCC was significantly associated with tumor differentiation, tumor size and microvascular invasion (Table 2). None of the seven well-differentiated HCC were detected by PET. The mean maximum standardized uptake value (SUVmax) (± SD) was 4.7 ± 1.3 in moderately differentiated HCC with positive PET findings, 5.7 ± 2.3 in poorly differentiated HCC and 26.2 in undifferentiated HCC. One poorly differentiated HCC with a maximum diameter of 17.0 cm, direct invasion to the stomach, and lymph node and pulmonary metastases, had a high SUVmax of 11.3. Moderately differentiated HCC with sarcomatous change had a high SUVmax of 18.6, and poorly differentiated HCC with sarcomatous change also showed high FDG uptake (SUVmax 14.1 and 25.0) (Fig. 1). One poorly differentiated HCC with sarcomatous change had a high SUVmax of 14.1 despite the small size of the tumor (1.6 cm) and absence of microvascular invasion

(Fig. 2). The patients with poorly differentiated HCC with sarcomatous change developed recurrences soon after surgery. One patient with an SUVmax of 14.1 had metastasis to the mediastinal lymph nodes 9 months after surgery, and another with an SUVmax of 25.0 developed intrahepatic metastasis 44 days after surgery.

Patients with cHCC-CC

Patient characteristics are summarized in Table 3. All three cHCC-CC were detected by PET and the SUVmax
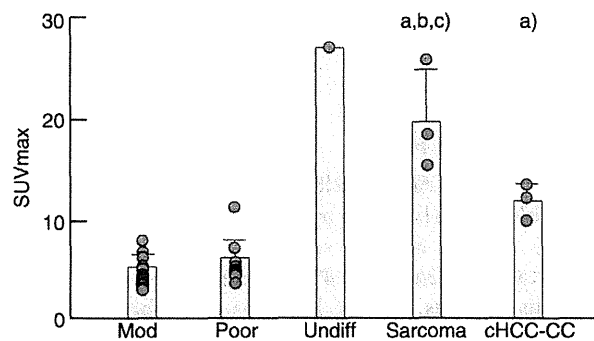

Figure 1 Maximum standardized uptake value (SUVmax) values of hepatocellular carcinoma (HCC) and combined hepatocellular and cholangiocarcinoma (cHCC-CC) with positive positron emission tomography (PET) findings. Undifferentiated HCC, moderately or poorly differentiated HCC with sarcomatous change, and cHCC-CC have high SUVmax values (>9.9), respectively. Data are expressed as mean ± standard deviation. (a) $P < 0.05$ vs mod; (b) $P < 0.05$ vs poor; (c) $P < 0.05$ vs cHCC-CC. Mod, moderately differentiated HCC; poor, poorly differentiated HCC; undiff, undifferentiated HCC; sarcoma, moderately or poorly differentiated HCC with sarcomatous change.
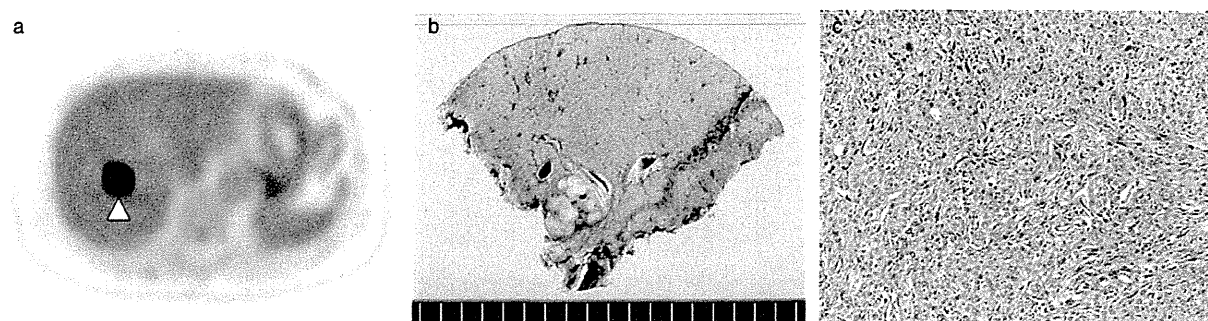
© 2012 The Japan Society of Hepatology

Figure 2 A 74-year-old female patient with poorly differentiated hepatocellular carcinoma (HCC) with sarcomatous change. (a) ^{18}F-Fluorodeoxyglucose positron emission tomography/computed tomography (FDG-PET/CT) image shows a liver mass with a maximum standardized uptake value (SUVmax) of 14.1 (arrow head). (b) Macroscopic image of the liver mass. (c) The liver tumor demonstrates histological features of poorly differentiated HCC with sarcomatous change (hematoxylin–eosin, original magnification ×100).

of cHCC-CC was 9.9, 12.0 and 13.0 (Fig. 1). One cHCC-CC had a high FDG uptake (SUVmax 12.0) despite the small size of the tumor (2.2 cm) and low levels of tumor markers (patient no. 1) (Fig. 3).

DISCUSSION

THE ROLE OF FDG PET/CT in the diagnosis and staging of HCC and other forms of liver cancer has been demonstrated in several reports.[6,7,19] However, preoperative evaluation of sarcomatous HCC and cHCC-CC with FDG PET/CT has not been reported so far. In the present study, we showed that sarcomatous HCC and cHCC-CC could be detected by PET/CT with high FDG uptake, and positive preoperative FDG uptake in HCC was significantly associated with tumor differentiation, tumor size and microvascular invasion.

Recently, several studies have shown that FDG-PET is useful for predicting tumor characterization, clinical outcome and prognosis in patients with HCC. Well-differentiated HCC regions were reported to show a tendency toward negativity by PET, whereas poorly differentiated types show increased FDG accumulation.[6,7] Our data also demonstrate that well-differentiated and some moderately differentiated HCC do not show FDG uptake exceeding that of the surrounding normal liver, whereas poorly differentiated and undifferentiated HCC have positive PET findings. There was no significant difference between the mean SUVmax of poorly differentiated HCC and that of moderately differentiated HCC with positive PET findings. On the other hand, the SUVmax of sarcomatous HCC were 18.6, 14.1 and 25.0, much higher than that of poorly differentiated HCC.

Table 3 Characteristics of patients with cHCC-CC

Characteristic	Patient no. 1	Patient no. 2	Patient no. 3
Age (years)/sex	78/M	54/M	47/M
Viral infection	HBsAg positive	Negative	HCVAb positive
Maximal tumor size (cm)	2.2	12.3	4.0
Microvascular invasion	Positive	Positive	Positive
Tumor stage (UICC)	II	IV	III
AFP (ng/mL)	4.3	16.4	18 286
DCP (mAU/mL)	20	45	231
CEA (ng/mL)	1.7	0.5	2.8
CA19-9 (U/mL)	7.4	76.6	31.9
Maximum SUV	12.0	9.9	13.0

CA19-9, carbohydrate antigen 19-9; CEA, carcinoembryonic antigen; DCP, des-γ-carboxy prothrombin; HBsAg, hepatitis B surface antigen; HCVAb, anti-hepatitis C virus antibody; SUV, standardized uptake value; UICC, Union for International Cancer Control.
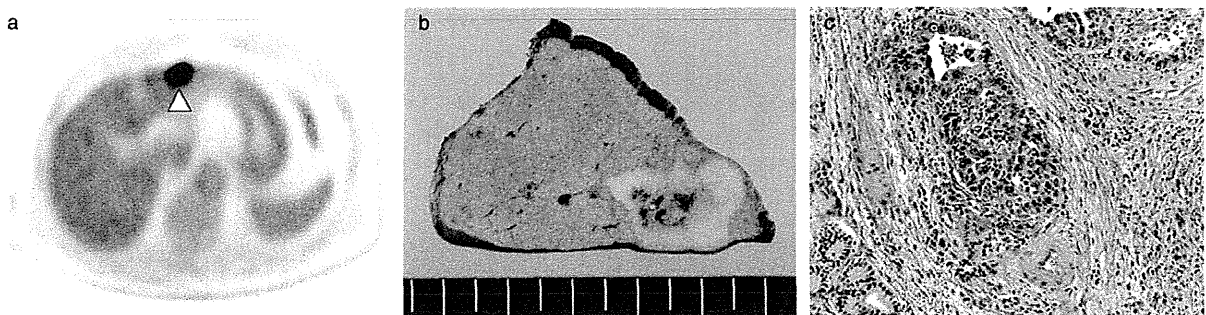
© 2012 The Japan Society of Hepatology

Figure 3 A 78-year-old male patient with combined hepatocellular and cholangiocarcinoma (cHCC-CC). (a) ^{8}F-Fluorodeoxyglucose positron emission tomography/computed tomography (FDG-PET/CT) image shows a liver mass with a maximum standardized uptake value (SUVmax) of 12.0 (arrow head). (b) Macroscopic image of the liver mass. (c) The liver tumor demonstrates histological features of cHCC-CC with microvascular invasion (hematoxylin–eosin, original magnification ×100).

Sarcomatous HCC is a rare histological variant of HCC.[13] Although the pathogenesis of sarcomatous HCC has not been clarified, the sarcomatous components are thought to be derived from a dedifferentiation or anaplasia, rather than from a combination of HCC and sarcoma.[13,20] Previous reports have suggested that anticancer therapy has an influence on the development of sarcomatous features in HCC, and the prognosis of patients with sarcomatous HCC is very poor due to frequent widespread metastases.[13,14,21] Although we performed curative resection for primary sarcomatous HCC, two of the three patients developed recurrences soon after surgery. Honda *et al.* reported that sarcomatous HCC appears as an irregularly demarcated intrahepatic mass with delayed or prolonged peripheral enhancement on CT.[22] However, it seemed to be difficult to make a correct preoperative diagnosis of sarcomatous changes by imaging or serological tumor markers. Our results show that FDG-PET may be a useful diagnostic tool for sarcomatous changes of HCC because the high FDG uptake of sarcomatous HCC seems to be related to its progression or aggressiveness.

In the present study, the SUVmax values of three cHCC-CC were higher than those of the poorly differentiated HCC. cHCC-CC is an uncommon subtype of primary liver cancer that contains elements of both HCC and CC.[15] Several studies have reported that the prognosis of patients with cHCC-CC was worse than that of patients with HCC because of frequent portal venous invasion and metastasis to lymph nodes and other organs.[16,17] Vascular invasion, tumor size and tumor stage were found to be prognostic factors for poor outcome in patients with

cHCC-CC.[16,23] Moreover, recent studies have demonstrated that a large CC component in cHCC-CC and a high serum carbohydrate antigen 19-9 (CA19-9) level were also associated with poorer survival rates.[24,25] We demonstrated that one cHCC-CC showed high FDG uptake (SUVmax 12.0) despite the low CA19-9 level (7.4 U/mL) and small size of the tumor (2.2 cm) (patient no. 1). In addition, another cHCC-CC showed high FDG uptake (SUVmax 13.0) despite the small CC component in the tumor (1%) (patient no. 3) (data not shown). If the degree of FDG uptake in cHCC-CC also reflects the aggressiveness of the tumor like other malignant tumors, FDG-PET may become a useful diagnostic tool for the preoperative evaluation of cHCC-CC.

Our data show that the SUVmax of sarcomatous HCC and cHCC-CC are much higher than those of liver cancers reported to be associated with poor prognosis in previous studies. Seo *et al.* have demonstrated that high FDG uptake (SUVmax ≥5.0) was a predictive factor of postoperative early recurrence and poor survival in patients with HCC.[7] Riedl *et al.* have also reported that an SUVmax of 5.0 or greater was correlated with worse long-term prognosis after liver resection for colorectal metastases.[26]

In summary, our studies demonstrate that FDG-PET shows high FDG uptake in sarcomatous HCC and cHCC-CC that have been reported to be associated with poor prognosis after surgery. Therefore, FDG-PET may be an effective diagnostic tool for the non-invasive evaluation of the aggressiveness of primary liver cancer before surgical resection and liver transplantation. Further clinical studies are warranted.

REFERENCES

1 Rigo P, Paulus P, Kaschten BJ *et al.* Oncological application of positron emission tomography with fluorine-18 fluoro-deoxyglucose. *Eur J Nucl Med* 1996; **23**: 1641–74.

2 Iglehart JK. The new era of medical imaging – progress and pitfalls. *N Engl J Med* 2006; **354**: 2822–8.

3 Trojan J, Schroeder O, Raedle J *et al.* Fluorine-18 FDG positron emission tomography for imaging of hepatocellular carcinoma. *Am J Gastroenterol* 1999; **94**: 3314–9.

4 Khan MA, Combs CS, Brunt EM *et al.* Positron emission tomography scanning in the evaluation of hepatocellular carcinoma. *J Hepatol* 2000; **32**: 792–7.

5 Torizuka T, Tamaki N, Inokuma T *et al.* In vivo assessment of glucose metabolism in hepatocellular carcinoma with FDG-PET. *J Nucl Med* 1995; **36**: 1811–7.

6 Hatano E, Ikai I, Higashi T *et al.* Preoperative positron emission tomography with fluorine-18-fluorodeoxy-glucose is predictive of prognosis in patients with hepatocellular carcinoma after resection. *World J Surg* 2006; **30**: 1736–41.

7 Seo S, Hatano E, Higashi T *et al.* Fluorine-18-fluorodeoxyglucose positron emission tomography predicts tumor differentiation, P-glycoprotein expression, and outcome after resection in hepatocellular carcinoma. *Clin Cancer Res* 2007; **13**: 427–33.

8 Ng IO. Prognostic significance of pathological and biological factors in hepatocellular carcinoma. *J Gastroenterol Hepatol* 1998; **13**: 666–70.

9 Kudo M. Multistep human hepatocarcinogenesis: correlation of imaging with pathology. *J Gastroenterol* 2009; **44** (Suppl 19): 112–8.

10 Sato M, Watanabe Y, Lee T *et al.* Well-differentiated hepatocellular carcinoma: clinicopathological features and results of hepatic resection. *Am J Gastroenterol* 1995; **90**: 112–6.

11 Oishi K, Itamoto T, Amano H *et al.* Clinicopathologic features of poorly differentiated hepatocellular carcinoma. *J Surg Oncol* 2007; **95**: 311–6.

12 Ikebe T, Wakasa K, Sasaki M *et al.* Hepatocellular carcinoma with chondrosarcomatous variation: case report with immunohistochemical findings, and review of the literature. *J Hepatobiliary Pancreat Surg* 1998; **5**: 217–20.

13 Maeda T, Adachi E, Kajiyama M, Takenaka K, Sugimachi K, Tsuneyoshi M. Spindle cell hepatocellular carcinoma: a clinicopahtologic and immunohistochemical analysis of 15 cases. *Cancer* 1996; **77**: 51–7.

14 Tsujimoto M, Aozasa K, Nakajima Y, Kariya M. Hepatocellular carcinoma with sarcomatous proliferation showing an unusual and widespread metastasis. *Acta Pathol Jpn* 1984; **34**: 839–45.

15 Primary liver cancer in Japan. Clinicopathologic features and results of surgical treatment. Liver Cancer Study Group of Japan. *Ann Surg* 1990; **211**: 277–87.

16 Jarnagin WR, Weber S, Tickoo SK *et al.* Combined hepatocellular and cholangiocarcinoma: demographic, clinical, and prognostic factors. *Cancer* 2002; **94**: 2040–6.

17 Yano Y, Yamamoto J, Kosuge T *et al.* Combined hepatocellular and cholangiocarcinoma: a clinicopathologic study of 26 resected cases. *Jpn J Clin Oncol* 2003; **33**: 283–7.

18 Nishie A, Yoshimitsu K, Asayama Y *et al.* Detection of combined hepatocellular and cholangiocarcinomas on enhanced CT: comparison with histologic findings. *Am J Roentgenol* 2005; **184**: 1157–62.

19 Breitenstein S, Apestegui C, Clavien PA. Positron emission tomography (PET) for cholangiocarcinoma. *HPB* 2008; **10**: 120–1.

20 Kakizoe S, Kojiro M, Nakashima T. Hepatocellular carcinoma with sarcomatous change: clinicopathologic and immunohistochemical studies of 14 autopsy cases. *Cancer* 1987; **59**: 310–6.

21 Kojiro M, Sugihara S, Kakizoe S, Nakashima O, Kiyomatsu K. Hepatocellular carcinoma with sarcomatous change: a special reference to relationship with anticancer therapy. *Cancer Chemother Pharmacol* 1989; **23**: 4–8.

22 Honda H, Hayashi T, Yoshida K *et al.* Hepatocellular carcinoma with sarcomatous change: characteristic findings of two-phased incremental CT. *Abdom Imaging* 1996; **21**: 37–40.

23 Koh KC, Lee H, Choi MS *et al.* Clinicopathologic features and prognosis of combined hepatocellular cholangiocarcinoma. *Am J Surg* 2005; **189**: 120–5.

24 Aishima S, Kuroda Y, Asayama Y *et al.* Prognostic impact of cholangiocellular and sarcomatous components in combined hepatocellular and cholangiocarcinoma. *Hum Pathol* 2006; **47**: 283–91.

25 Kim KH, Lee SG, Park EH *et al.* Surgical treatments and prognosis of patients with combined hepatocellular carcinoma and cholangiocarcinoma. *Ann Surg Oncol* 2009; **16**: 623–9.

26 Riedl CC, Akhurst T, Larson S *et al.* 18F-FDG PET scanning correlates with tissue markers of poor prognosis and predicts mortality for patients after liver resection for colorectal metastases. *J Nucl Med* 2007; **48**: 771–5.

Rendezvous Ductoplasty for Biliary Anastomotic Stricture After Living-Donor Liver Transplantation

Shohei Yoshiya, Ken Shirabe, Yoshihiro Matsumoto, Tetsuo Ikeda, Yuji Soejima, Tomoharu Yoshizumi Hideaki Uchiyama, Toru Ikegami, Norifumi Harimoto, and Yoshihiko Maehara

Background. Biliary anastomotic stricture (BAS) after living-donor liver transplantation (LDLT) is difficult to manage. We used rendezvous ductoplasty (RD) to treat BAS after LDLT.

Methods. We retrospectively analyzed 53 patients with BAS after adult-to-adult LDLT with duct-to-duct biliary reconstruction.

Results. BAS was classified according to endoscopic retrograde cholangiography findings after normal-pressure contrast injection: type I (n=32) in which the stricture was visualized; type II (n=13) in which the common hepatic duct and graft intrahepatic ducts were visualized, but the stricture was not visualized; or type III (n=8) in which the stricture and graft intrahepatic ducts were not visualized. In right lobe grafts, types II and III occurred more frequently than type I (P=0.0023). Type I had significantly shorter cold ischemic time (76±11 vs. 118±12 min; P=0.0155) and warm ischemic time (38±2 vs. 49±3 min; P=0.0069) than types II and III. The number of attempts to pass the guidewire through the stricture was significantly lower in type I (1.2±0.2 attempts) than type II (2.2±0.2 attempts; P=0.0018) or type III (2.8±0.3 attempts; P<0.0001). The treatment success rate was 78.1% for type I, 38.5% for type II, and 50.0% for type III (P=0.0282). RD was the first successful treatment in a higher proportion of types II and III patients than type I patients (66.7% vs. 6.3%; P<0.0001). Cumulative treatment success rates were not significantly different between the RD and the non-RD groups (P=0.0920).

Conclusions. RD was a useful treatment for difficult cases of BAS after LDLT and achieved successful outcomes.

Keywords: Living-donor liver transplantation, Biliary anastomotic stricture, ERC, PTC.

L iving-donor liver transplantation (LDLT) is one of the treatment options for end-stage liver disease, especially in countries with a shortage of deceased donors. Duct-to-duct biliary reconstruction, which preserves biliary function, is now preferred over hepaticojejunostomy (1–4). Biliary complications, including biliary anastomotic stricture (BAS), are the most common complications after LDLT and have been reported to occur in 19% of LDLT patients (5, 6). BAS treatment is difficult and requires frequent and prolonged hospitalizations, resulting in loss of quality of life (2).

Currently, many institutes manage BAS via the endoscopic transpapillary approach, but this approach has a failure rate of more than 40% (7). The percutaneous transhepatic approach may be used as second-line treatment (4, 8, 9). Surgery may be considered when other modalities have failed and may include conversion from duct-to-duct anastomosis to hepaticojejunostomy. However, surgical treatment carries a risk of related complications (10), and a nonsurgical approach is therefore preferable when reasonable results can be expected.

We performed rendezvous ductoplasty (RD; Fig. 1) in patients with BAS who were difficult to manage. The aims of this study were to classify BAS, to evaluate the difficulty of treatment according to BAS type, and to evaluate the usefulness of RD for treating BAS.

RESULTS

BAS Classification

To evaluate the difficulty of passing a guidewire through the stricture, we classified BAS into three types according to cholangiography findings after normal-pressure contrast injection. In type I, the common hepatic duct, stricture, and graft intrahepatic ducts were visualized (Fig. 2A). In type II, the common hepatic duct and graft intrahepatic ducts were visualized, but the area of the stricture was not visualized (Fig. 2B). In type III, the common hepatic duct was visualized,
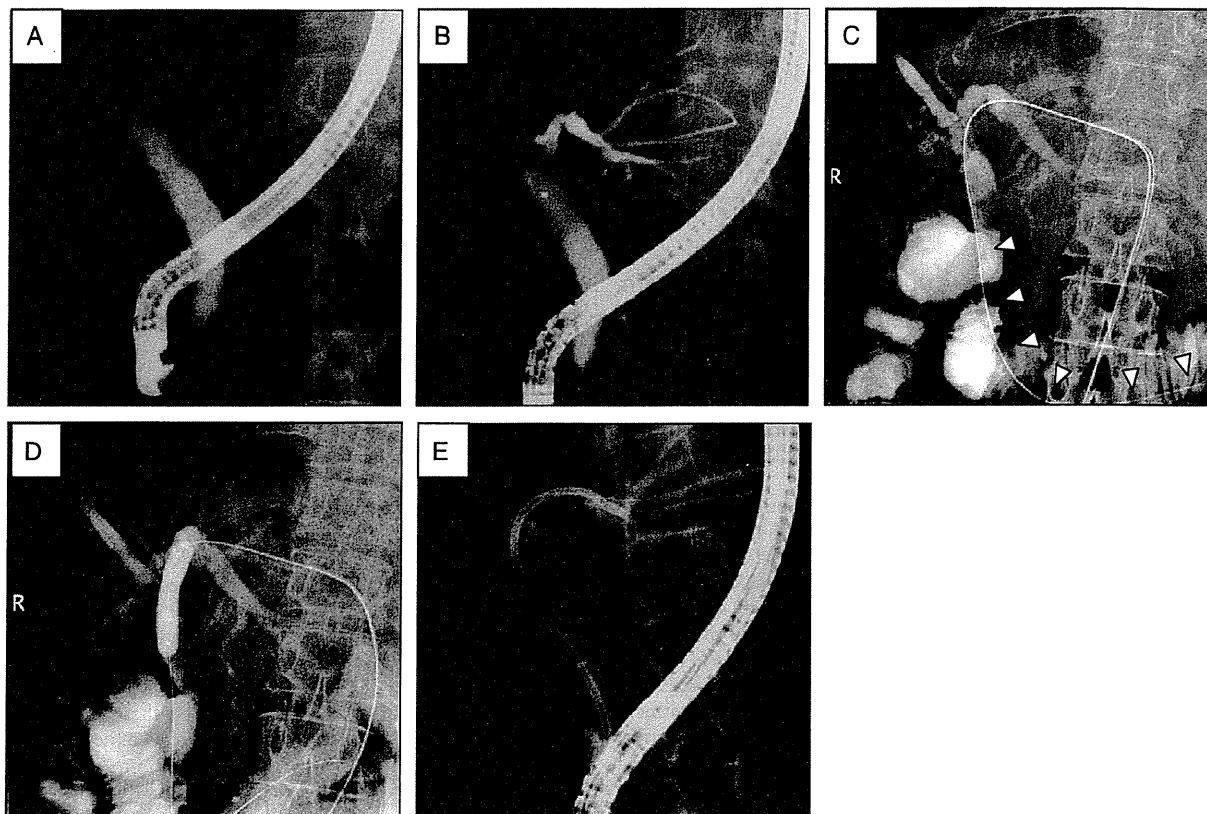
FIGURE 1. RD procedure. A, endoscopic access in the prone position. B, percutaneous transhepatic access under fluoroscopic guidance with endoscopic contrast agent injection. C, guidewire is passed from the percutaneous transhepatic side through the stricture and the ampulla of Vater. D, E, balloon dilatation followed by stent placement using the endoscope. RD, rendezvous ductoplasty.

but the area of the stricture and the graft intrahepatic ducts were not visualized (Fig. 2C).

Clinical Characteristics in the Three Types of BAS

Analysis of variance showed a significant association between graft type and BAS type. Among patients with type I BAS, 24 had left lobe (LL) grafts, 8 had right lobe (RL) grafts, and none had posterior segment (PS) grafts; among patients with type II BAS, 4 had LL grafts, 8 had RL grafts, and 1 had a PS graft; and among patients with type III BAS, 3 had LL grafts, 3 had RL grafts, and 2 had PS grafts ($P=0.0079$). There were significant differences among types I to III in cold ischemic time (76 ± 11 vs. 131 ± 16 vs. 98 ± 20 min; $P=0.0240$) and warm ischemic time (38 ± 2 vs. 54 ± 3 vs. 40 ± 4 min; $P=0.0015$). In addition, Tukey–Kramer's tests revealed significant differences between types I and II in cold ischemic time ($P=0.0011$) and warm ischemic time ($P=0.0431$). Multivariate analyses comparing types I and II showed that warm ischemic time was an independent risk factor for type II (odds ratio, 1.17; 95% confidence interval, 0.70–0.96; $P=0.0030$). Multivariate analyses comparing types I and III showed that an RL graft was an independent risk factor for type III compared with an LL graft (odds ratio, 5.00; 95% confidence interval, 1.01–29.24; $P=0.0491$). There were no significant differences

among BAS types in the rates of hepatitis C virus infection ($P=0.5933$) or other recipient factors, donor factors, operative factors, or postoperative factors (Table 1).

Evaluation of Difficulty of Treatment in the Three Types of BAS

We evaluated the difficulty of treatment in the three types of BAS using two factors: the number of attempts to pass the guidewire through the stricture and the rate of successful completion of treatment. The number of attempts to pass the guidewire was significantly lower in type I than type II (1.2 ± 0.2 vs. 2.2 ± 0.2 attempts; $P=0.0018$) or type III (1.2 ± 0.2 vs. 2.8 ± 0.3 attempts; $P<0.0001$), but there was no significant difference in the number of attempts between types II and III (Table 1). The rate of successful treatment was 78.1% in type I, 38.5% in type II, and 50.0% in type III ($P=0.0282$).

First Successful Treatment Modality in Each Type of BAS

We analyzed the first successful treatment modality in each type of BAS. Overall, we performed endoscopic retrograde cholangiography (ERC), percutaneous transhepatic cholangiography (PTC), and RD in 66.0% (n=35), 3.8% (n=2), and 30.2% (n=16) of cases, respectively (Fig. 3A). In type I, we performed ERC, PTC, and RD in 87.4% (n=28), 6.3% (n=2), and 6.3% (n=2) of cases, respectively (Fig. 3B). In type II, we
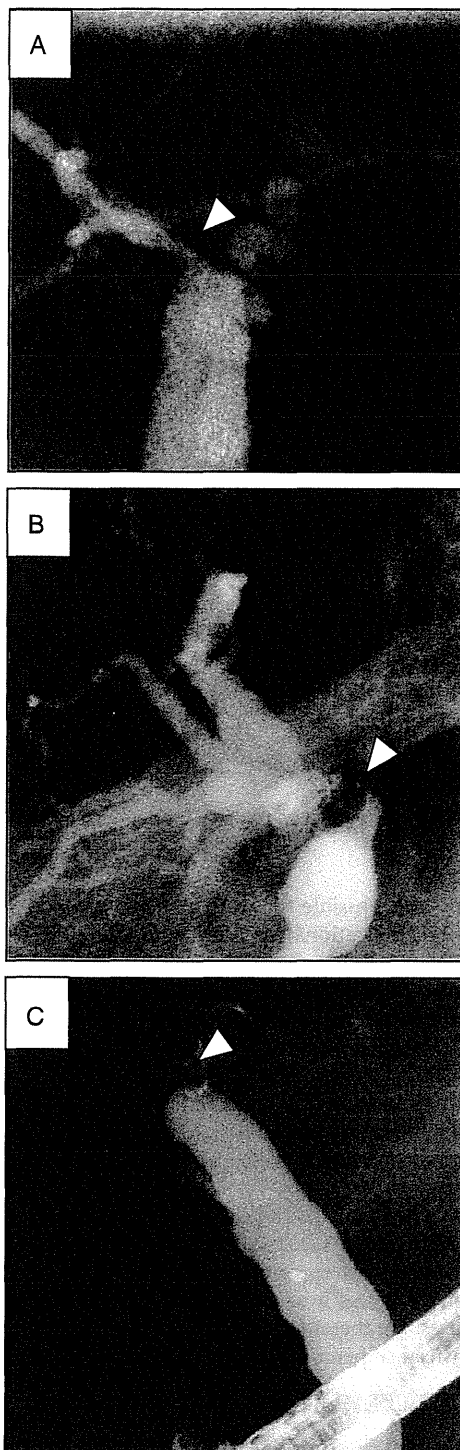
FIGURE 2. Three types of BAS according to cholangiography findings. A, type I, with the narrow stricture visualized. B, type II, with the common hepatic duct and graft intrahepatic ducts visualized, but the stricture not visualized. C, type III, with the stricture and the donor intrahepatic ducts not visualized. Arrowheads indicate the stricture site. BAS, biliary anastomotic stricture.

performed ERC, PTC, and RD in 46.2% (n=6), 0% (n=0), and 53.8% (n=7) of cases, respectively (Fig. 3C). In type III, we performed ERC, PTC, and RD in 12.5% (n=1), 0% (n=0), and 87.5% (n=7) of cases, respectively (Fig. 3D). The rate of RD was significantly higher in types II and III than type I (66.7% vs. 6.3%; $P<0.0001$).

Comparison of Cumulative Treatment Success Rates between the RD and the Non-RD Groups

To evaluate the usefulness of RD, we divided patients into two groups: an RD group (n=16) and a non-RD group (n=37). The 1- and 4-year cumulative treatment success rates were 26.7% and 87.6%, respectively, in the RD group and 51.3% and 89.0%, respectively, in the non-RD group (Fig. 4). The cumulative success rates were not significantly different between the two groups (P=0.0920). None of the 53 patients with BAS underwent surgical treatment.

DISCUSSION

Although efforts to prevent BAS have decreased the frequency of this complication, from 14.5% to 32.5% of patients who receive LDLT still develop BAS (1, 3, 11–13). Development of BAS is related to various factors, such as the fragile vascular networks in the biliary tree, ischemia-reperfusion injury, age-related changes, fibrous scar formation as part of the normal healing process, tiny or multiple bile duct orifices, and immunologic reactions (1, 12, 14, 15). We focused on careful dissection of the peribiliary tissues to preserve maximal vascular integrity of the recipient's bile duct and achieved a BAS rate of 14.5%, which is lower than the rate of 32.5% reported in the literature (1, 16). However, other factors causing BAS have not been overcome, and BAS is still thought to be an inevitable complication after LDLT.

In this study, BAS was classified into three types according to cholangiography findings, and the difficulty of treating each type was evaluated. Lee et al. (13) reported that stricture morphology was a significant factor ($P<0.0001$) in the success rate of primary endoscopic management. Kato et al. (2) reported that cholangiography findings were related to the risk of failure of stent deployment. However, no studies have reported on the difficulty of treatment according to BAS type.

The current study found that graft type, cold ischemic time, and warm ischemic time were associated with BAS type after LDLT. Previous studies reported that the incidence of BAS was higher in RL grafts than LL grafts because of the anatomy of the right bile duct (3, 15, 17–19). Graft stumps tend to be more horizontal in PS grafts than RL grafts. Interestingly, there were no cases of type I BAS in patients with PS grafts in this study, which suggests that both bile duct size and the biliary anastomotic angle have an effect on BAS type. Although cold ischemic time was not significantly associated with BAS in our series, it is thought to induce postreperfusion endothelial damage, resulting in impaired perfusion (1). Warm ischemic time has also been reported to be a risk factor for BAS after LDLT because of its impact on graft microcirculation (12, 20). We therefore assumed an association between the microcirculation around the biliary tree and BAS type. Other reported risk factors for BAS, such as hepatic artery flow (21) and biliary leakage (1, 15, 22), were not significantly associated with BAS type in this series.

TABLE 1. Patient characteristics by type of BAS after LDLT

	Type I (n=32)	Type II (n=13)	Type III (n=8)	P
Recipient factors				
Age, yr	57.1 ± 1.5	56.3 ± 2.3	57.9 ± 2.9	0.9109
Gender, male (%)	19 (59.4)	9 (69.2)	3 (37.5)	0.3544
MELD score, points	14.9 ± 0.0	18.2 ± 1.4	16.3 ± 1.8	0.1409
Hepatitis C virus infection (%)	21 (65.6)	7 (53.9)	6 (75.0)	0.5933
Donor factors				
ABO-incompatible graft (%)	1 (3.1)	1 (7.7)	1 (12.5)	0.5477
Graft type (LL/RL/PS)	24/8/0	4/8/1	3/3/2	0.0079[a]
GV/SLV (%)	40.1 ± 1.2	45.5 ± 1.9	39.7 ± 2.4	0.0740
Operative factors				
Operation time, min	750 ± 31	848 ± 49	785 ± 62	0.2458
Cold ischemic time, min	76 ± 11	131 ± 16	98 ± 20	0.0240[a]
Warm ischemic time, min	38 ± 2	54 ± 3	40 ± 4	0.0015[a]
Operative blood loss, L	6.12 ± 1.21	5.76 ± 1.89	4.19 ± 2.41	0.7680
HAF at closure, mL/min	90 ± 9	91 ± 15	96 ± 19	0.9586
No. donor bile ducts (1/2/3)	25/6/1	11/2/0	7/1/0	0.8640
Bile ductoplasty (%)	9 (28.1)	4 (30.8)	2 (25.0)	0.9594
Postoperative factors				
Bile leakage (%)	4 (12.5)	3 (23.1)	2 (25.0)	0.5666
Time to biliary stricture, yr	0.95 ± 0.16	0.68 ± 0.26	0.87 ± 0.33	0.6700
Difficulty of treatment				
No. attempts	1.2 ± 0.2	2.2 ± 0.2	2.8 ± 0.3	<0.0001[a]
Treatment success rate (%)	25 (78.1)	5 (38.5)	4 (50.0)	0.0282[a]

[a] $P<0.05$.

BAS, biliary anastomotic stricture; GV, graft volume; HAF, hepatic artery flow; LDLT, living-donor liver transplantation; LL, left lobe graft; MELD, model for end-stage liver disease; PS, posterior segment; RL, right lobe; SLV, standard liver volume.

Because the current first-line therapy for BAS is endoscopic balloon dilatation and stent placement, passage of a guidewire through the stricture is critical (2, 8, 13). The success rate of primary endoscopic treatment is 40% to 90% (6), and percutaneous treatment may be performed as second-line therapy if endoscopic treatment has failed (4, 8, 9). However, it is difficult to access the intrahepatic duct using ultrasonography if it is not dilated. Giampalma et al. (23) reported a percutaneous treatment failure rate of 10% (5 of 48). When both endoscopic and percutaneous treatments have failed, surgical therapy is usually unavoidable (10).

When performing RD, we were easily able to access nondilated intrahepatic ducts after visualizing them with endoscopic contrast agent injection. We therefore assume that it is easier to treat BAS using RD than PTC. We were able to apply sufficient force to both ends of guidewire, via the patient's mouth and the transhepatic route, to enable us to align the stricture and place stents. Use of RD therefore avoided the need for external stents, which would have reduced quality of life. The duration of treatment tended to be shorter in the non-RD group than the RD group, but cumulative treatment success rates were not significantly different between the RD and the non-RD groups (P=0.0920). None of our patients required hepaticojejunostomy or repeat transplantation. These results indicate the importance of successful initial treatment of BAS after LDLT.

The main limitations of this study are its retrospective nature, possible biases due to the learning curves for surgical techniques, and possible biases in patient selection for RD. However, the indications for LDLT and our graft selection criteria were consistent. Another limitation is the relatively small number of cases. Although our findings support the use of RD for BAS after LDLT with duct-to-duct biliary reconstruction, they do not provide definitive evidence of the usefulness of BAS, because it was not possible to make direct comparisons between RD and control treatments. Further analysis of a larger number of patients in a multicenter study, such as a randomized controlled trial, is necessary to confirm our findings.

In conclusion, ERC findings predicted the difficulty of treatment of BAS after LDLT with duct-to-duct reconstruction. Most cases of BAS were successfully treated with endoscopic therapy, and RD was a useful treatment modality for more difficult cases. We therefore advocate using RD as second-line therapy instead of percutaneous transhepatic approach.

MATERIALS AND METHODS

Patients

Between June 2001 and July 2012, 289 LDLTs with duct-to-duct biliary reconstruction were performed at Kyushu University Hospital (Fukuoka, Japan). Fifty-three (18.3%) of these patients developed BAS and were included in this study.

Donor Surgery

The surgical techniques for graft harvesting have previously been described (24). From 2005, we performed minimal dissection around the bile duct to preserve the blood supply. Before 2005, we performed more extensive
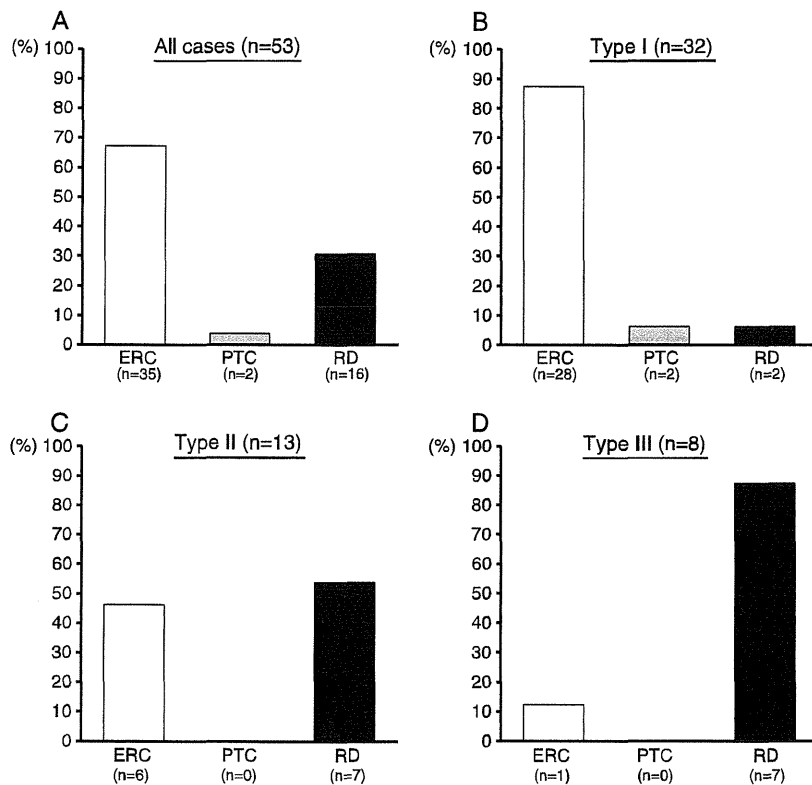
FIGURE 3. First successful treatment modalities in each type of BAS: (A) all cases, (B) type I cases, (C) type II cases, and (D) type III cases. BAS, biliary anastomotic stricture; ERC, endoscopic retrograde cholangiography; PTC, percutaneous transhepatic cholangiography; RD, rendezvous ductoplasty.

dissection of the tissues surrounding the bile duct. After complete parenchymal transection, we performed intraoperative fluorocholangiography to examine the anatomical details of the biliary ducts and determine the location and angle for hepatic duct transection. Intraoperative fluorocholangiography was performed with a portable C-arm unit (Arcadis Avantic; Siemens, Berlin, Germany) from 2005 and with a static X-ray film unit before 2005. Ductoplasty was sometimes performed during the cold phase if multiple bile ducts were located close together in the graft.

Recipient Surgery

We introduced duct-to-duct biliary reconstruction in 2001 (*25*). From April 2006, we used the minimal hilar dissection technique (*1*, *16*) to preserve maximal vascular integrity of the recipient biliary tree. Before April 2005, we dissected the peribiliary connective tissues to isolate the common bile duct. After portal and arterial reconstruction, biliary reconstruction was performed as follows. Interrupted 6-0 absorbable monofilament sutures were placed over a straight silicone external stent tube (2.0–3.0 mm retrograde transhepatic biliary drainage tube; Sumitomo Bakelite, Tokyo, Japan) with the knots outside the lumen. The silicone stent tube was anchored at the biliary anastomosis and passed through the anterior wall of the recipient's common bile duct. Intraoperative fluorocholangiography was performed to confirm that there were no biliary strictures or leakages. The stent tube was removed in a two-step process under fluoroscopic guidance at least 3 months after surgery, as previously described (*26*). We have not changed our procedure since 2006.

Diagnosis and Treatment of BAS

Biliary stricture was suspected when a patient developed elevated liver enzyme levels or symptoms such as jaundice, itching, or fever. BAS was confirmed by direct imaging techniques such as ERC. The time of onset of BAS was defined as the day of diagnosis on imaging findings, and the completion

of treatment was defined as the day a stent-free state was achieved (free passage of injected contrast agent and good drainage from the intrahepatic duct on cholangiography). When BAS was diagnosed, endoscopic treatment was attempted first. If several attempts to pass the guidewire through the stricture failed, RD was performed. Biliary stents were changed endoscopically every
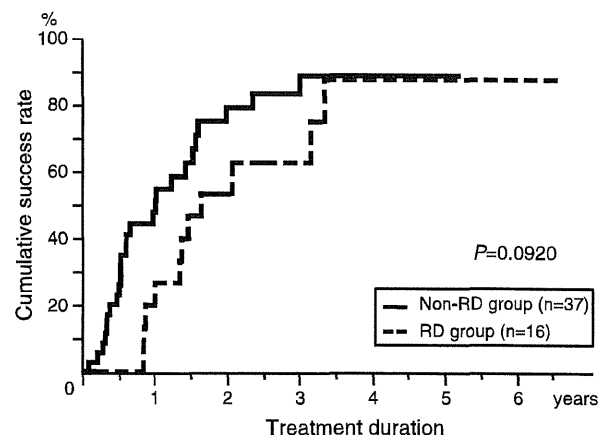

FIGURE 4. Cumulative 1- and 4-year treatment success rates were 26.7% and 87.6%, respectively, in the RD group (n=16) and 51.3% and 89.0%, respectively, in the non-RD group (n=37; *P*=0.0920). RD, rendezvous ductoplasty.

3 to 6 months, at which time the BAS was reevaluated. Stenting was continued until the stricture had resolved.

Endoscopic Transpapillary Approach Procedure

Our endoscopic transpapillary approach procedure was as follows. Under conscious sedation, the patient was placed prone and the ampulla of Vater was cannulated. Contrast agent was injected through the cannula to show the common hepatic duct and the graft intrahepatic ducts. If the graft intrahepatic ducts were not visible, we used balloon occlusion to increase the pressure of the contrast injection. We then tried to pass the guidewire through the stricture followed by balloon dilatation and stent placement.

RD Procedure

RD was performed as follows (Fig. 1). First, endoscopic access was obtained in the prone position. The patient was then placed supine, keeping the endoscope in position, and percutaneous transhepatic access was obtained under fluoroscopic guidance. If the intrahepatic ducts could not be visualized (type III), we used balloon occlusion to increase the pressure of the contrast agent injection. The guidewire from the percutaneous transhepatic side was passed through the stricture and through the ampulla of Vater. We then performed balloon dilatation before or after the guidewire was withdrawn through the mouth using the endoscope followed by stent placement as for the endoscopic transpapillary approach. If the guidewire could not be passed through the stricture during the RD procedure, we placed a temporary external drainage stent via the percutaneous transhepatic route to reduce duct edema. During subsequent RD sessions, we inserted the guidewire via the external drainage route and then attempted to pass it through the stricture. After RD, we usually removed the balloon via the percutaneous transhepatic route. We did not experience any cases of clinical bile leakage or biliary peritonitis.

Statistical Analysis

All statistical analyses were performed using SAS software (JMP 9.0.1; SAS Institute, Cary, NC). Multiple comparisons were performed using analysis of variance and Tukey–Kramer tests. Cumulative treatment success rates were analyzed using the Kaplan–Meier method and compared using the log-rank test. All variables are expressed as mean±standard deviation. $P<0.05$ was considered statistically significant.

REFERENCES

1. Ikegami T, Shirabe K, Morita K, et al. Minimal hilar dissection prevents biliary anastomotic stricture after living donor liver transplantation. *Transplantation* 2011; 92: 1147.
2. Kato H, Kawamoto H, Tsutsumi K, et al. Long-term outcomes of endoscopic management for biliary strictures after living donor liver transplantation with duct-to-duct reconstruction. *Transpl Int* 2009; 22: 914.
3. Kasahara M, Egawa H, Takada Y, et al. Biliary reconstruction in right lobe living-donor liver transplantation: comparison of different techniques in 321 recipients. *Ann Surg* 2006; 243: 559.
4. Wang SF, Huang ZY, Chen XP. Biliary complications after living donor liver transplantation. *Liver Transpl* 2011; 17: 1127.
5. Traina M, Tarantino I, Barresi L, et al. Efficacy and safety of fully covered self-expandable metallic stents in biliary complications after liver transplantation: a preliminary study. *Liver Transpl* 2009; 15: 1493.
6. Akamatsu N, Sugawara Y, Hashimoto D. Biliary reconstruction, its complications and management of biliary complications after adult liver transplantation: a systematic review of the incidence, risk factors and outcome. *Transpl Int* 2011; 24: 379.
7. Sharma S, Gurakar A, Jabbour N. Biliary strictures following liver transplantation: past, present and preventive strategies. *Liver Transpl* 2008; 14: 759.
8. Balderramo D, Sendino O, Burrel M, et al. Risk factors and outcomes of failed endoscopic retrograde cholangiopancreatography in liver transplant recipients with anastomotic biliary strictures: a case-control study. *Liver Transpl* 2012; 18: 482.
9. Kim ES, Lee BJ, Won JY, et al. Percutaneous transhepatic biliary drainage may serve as a successful rescue procedure in failed cases of endoscopic therapy for a post-living donor liver transplantation biliary stricture. *Gastrointest Endosc* 2009; 69: 38.
10. Reichman TW, Sandroussi C, Grant DR, et al. Surgical revision of biliary strictures following adult live donor liver transplantation: patient selection, morbidity, and outcomes. *Transpl Int* 2012; 25: 69.
11. Lee KW, Joh JW, Kim SJ, et al. High hilar dissection: new technique to reduce biliary complication in living donor liver transplantation. *Liver Transpl* 2004; 10: 1158.
12. Chok KS, Chan SC, Cheung TT, et al. Bile duct anastomotic stricture after adult-to-adult right lobe living donor liver transplantation. *Liver Transpl* 2011; 17: 47.
13. Lee YY, Gwak GY, Lee KH, et al. Predictors of the feasibility of primary endoscopic management of biliary strictures after adult living donor liver transplantation. *Liver Transpl* 2011; 17: 1467.
14. Liu CL, Lo CM, Chan SC, et al. Safety of duct-to-duct biliary reconstruction in right-lobe live-donor liver transplantation without biliary drainage. *Transplantation* 2004; 77: 726.
15. Shah SA, Grant DR, McGilvray ID, et al. Biliary strictures in 130 consecutive right lobe living donor liver transplant recipients: results of a western center. *Am J Transplant* 2007; 7: 161.
16. Soejima Y, Taketomi A, Yoshizumi T, et al. Biliary strictures in living donor liver transplantation: incidence, management, and technical evolution. *Liver Transpl* 2006; 12: 979.
17. Ohkubo M, Nagino M, Kamiya J, et al. Surgical anatomy of the bile ducts at the hepatic hilum as applied to living donor liver transplantation. *Ann Surg* 2004; 239: 82.
18. Hwang S, Lee SG, Sung KB, et al. Long-term incidence, risk factors, and management of biliary complications after adult living donor liver transplantation. *Liver Transpl* 2006; 12: 831.
19. Ikegami T, Soejima Y, Shirabe K, et al. Evolving strategies to prevent biliary strictures after living donor liver transplantation. *Transplant Proc* 2010; 42: 3624.
20. Puhl G, Schaser KD, Pust D, et al. The delay of rearterialization after initial portal reperfusion in living donor liver transplantation significantly determines the development of microvascular graft dysfunction. *J Hepatol* 2004; 41: 299.
21. Hashimoto K, Miller CM, Quintini C, et al. Is impaired hepatic arterial buffer response a risk factor for biliary anastomotic stricture in liver transplant recipients? *Surgery* 2010; 148: 582.
22. Park JB, Kwon CH, Choi GS, et al. Prolonged cold ischemic time is a risk factor for biliary strictures in duct-to-duct biliary reconstruction in living donor liver transplantation. *Transplantation* 2008; 86: 1536.
23. Giampalma E, Renzulli M, Mosconi C, et al. Outcome of post-liver transplant ischemic and nonischemic biliary stenoses treated with percutaneous interventions: the Bologna experience. *Liver Transpl* 2012; 18: 177.
24. Taketomi A, Morita K, Toshima T, et al. Living donor hepatectomies with procedures to prevent biliary complications. *J Am Coll Surg* 2010; 211: 456.
25. Soejima Y, Shimada M, Suehiro T, et al. Feasibility of duct-to-duct biliary reconstruction in left-lobe adult-living-donor liver transplantation. *Transplantation* 2003; 75: 557.
26. Eguchi S, Takatsuki M, Hidaka M, et al. Two-step external stent removal after living donor liver transplantation. *Transpl Int* 2008; 21: 531.

Obstructing Spontaneous Major Shunt Vessels is Mandatory to Keep Adequate Portal Inflow in Living-Donor Liver Transplantation

Toru Ikegami, Ken Shirabe, Hidekazu Nakagawara, Tomoharu Yoshizumi, Takeo Toshima, Yuji Soejima, Hideaki Uchiyama, Yo-Ichi Yamashita, Norifumi Harimoto, and Yoshihiko Maehara

Background. It has not been addressed whether the major spontaneous portosystemic shunt vessels should be ligated in living-donor liver transplantation (LDLT).
Methods. We performed a retrospective analysis of 324 cases of adult-to-adult LDLT.
Results. Factors associated with the presence of major (>10 mm) shunt vessels (n=130) included portal vein (PV) thrombosis (27.7%), lower PV pressure at laparotomy, Child-Pugh class C, and transplantation of right-side grafts. The types of major portosystemic shunt vessels included splenorenal shunts (46.2%), gastroesophageal shunts (26.9%), mesocaval shunts (13.8%), and others (13.1%). Ligation of the major shunt vessels increased PV pressure (mean [SD], from 16.8 [3.9] mm Hg to 18.6 [4.3] mm Hg; $P<0.001$) and PV flow (mean [SD], from 1.35 [0.67] L/min to 1.67 [0.67] L/min; $P<0.001$) into the grafts. Post-LDLT computed tomography showed patent major shunts in 14 patients. Nine of such patients (64.3%) with unligated major shunt vessels (undetected shunt vessels, n=5; incomplete ligation, n=2; and the shunt was newly created or left open to maintain high PV pressure after reperfusion, n=3) required secondary interventions. Two of these patients died because of graft dysfunction. PV flow was significantly lower in the nine patients who underwent secondary ligation of the major shunt vessels compared with patients with successful primary ligation (mean [SD], 0.96 [0.34] L/min vs. 1.65 [0.63] L/min; $P=0.001$).
Conclusions. It is an appropriate option to obstruct the major portosystemic shunt vessels to ensure adequate graft inflow in LDLT.

Keywords: Shunt vessels, Portal vein, Living-donor liver transplantation, Splenectomy.

(Transplantation 2013;95: 1270–1277)

Portal hypertension is a common outcome of end-stage liver disease, and it causes gastrointestinal bleeding, hypersplenism, intractable ascites, and hepatic encephalopathy (*1*). For treating such portal hypertension, transjugular intrahepatic portosystemic shunt has been commonly applied

Department of Surgery and Science, Graduate School of Medical Sciences, Kyushu University, Fukuoka, Japan.
Address correspondence to: Toru Ikegami, M.D., Department of Surgery and Science, Graduate School of Medical Sciences, Kyushu University, Fukuoka, Japan.
E-mail: tikesurg@ysurg2.med.kyushu-u.ac.jp

mainly in Western countries, resulting in uncommon development of tremendous or major shunt vessels (*2, 3*). In Eastern countries including Japan, however, transjugular shunting approach is less commonly used and replaced by other types of endoscopic or interventional treatment (*4, 5*), and therefore, patients who are referred for liver transplantation frequently have major portosystemic shunt vessels.

Liver transplantation is the ultimate treatment of portal hypertension, and it is known that splenomegaly and major spontaneous portosystemic shunts recover after whole-liver transplantation (*6–9*). On the other hand, after living-donor liver transplantation (LDLT), transient or persistent portal hypertension with increased portal vein (PV) resistance could occur even after surgery because of significant graft regeneration and small-for-size graft dysfunction (*10–12*). Thus, in LDLT recipients with major portosystemic shunt vessels, increased PV pressure might cause portal steal phenomenon, resulting in insufficient portal inflow and graft dysfunction (*13–15*).

In this study, we retrospectively analyzed 324 adult LDLT cases to determine the clinical characteristics of patients with major spontaneous portosystemic shunt vessels and, ultimately, to assess whether such major shunts need to be obstructed in LDLT.

RESULTS

Characteristics of the Recipients, Donors, and Grafts

The mean (SD) age of the recipients was 52.4 (11.3) years. Indications for LDLT included cholestatic cirrhosis (n=85, 26.2%), postnecrotic viral or nonviral cirrhosis (n=229, 70.7%), and others (n=10, 3.1%). Approximately half of the patients were hepatitis C virus positive (n=154, 47.5%). Almost two-third of the patients were classified as Child-Pugh class C (n=206, 63.6%). The mean (SD) model for end-stage liver disease score was 15.8 (6.1). Major shunt vessels were present in 130 recipients (40.1%). The mean (SD) age of the donors was 36.5 (11.3) years. Graft types included left-lobe (n=197, 60.8%), right-lobe (n=120, 37.0%), and posterior segment (n=7, 2.2%) grafts. Twelve donors (4.3%) provided blood type–incompatible grafts. The mean (SD) graft volume (GV) and GV/standard liver volume (SLV) were 478 (105) g

TABLE 1. Patient demographics

Variables	Presence of Major Shunt Vessels		
	No (n=194)	Yes (n=130)	P
Recipient age, mean (SD), y	51.9 (11.6)	53.0 (10.8)	0.409
Recipient gender, male, n (%)	104 (53.6)	56 (43.1)	0.063
Child-Pugh class C, n (%)	113 (58.2)	93 (71.5)	0.015
MELD score, mean (SD)	15.3 (6.6)	16.4 (5.3)	0.109
Hospitalized status, n (%)	68 (35.1)	44 (42.3)	0.187
PV thrombosis before LDLT, n (%)	8 (4.1)	36 (27.7)	<0.001
Hepatocellular carcinoma, n (%)	99 (51.9)	63 (48.5)	0.650
Donor age, mean (SD), y	36.9 (11.2)	35.9 (11.5)	0.407
Donor gender, male, n (%)	130 (67.0)	76 (58.5)	0.117
Blood type–incompatible donor, n (%)	7 (3.6)	7 (5.4)	0.447
Left-lobe graft, n (%)	131 (67.5)	66 (50.7)	0.002
GV, mean (SD), g	472 (106)	486 (104)	0.282
GV/SLV ratio, mean (SD), %	41.1 (8.5)	41.9 (8.4)	0.391
PV pressure at laparotomy, mean (SD), mm Hg	25.0 (5.8)	23.8 (5.4)	0.048
PV pressure at the closure, mean (SD), mm Hg	17.1 (4.2)	17.1 (4.3)	0.856
PV flow, mean (SD), L/min/graft	1.68 (0.40)	1.68 (0.65)	0.995
HA flow, mean (SD), mL/min	110 (70)	103 (68)	0.449
Operation time, mean (SD), min	802 (179)	813 (192)	0.585
Operative blood loss, mean (SD), L	8.4 (19.1)	6.6 (10.1)	0.305
Acute cellular rejection, n (%)	30 (15.4)	16 (12.3)	0.425
PV thrombosis, n (%)	3 (1.5)	5 (3.8)	0.190
Bacteremia, n (%)	21 (10.8)	18 (13.9)	0.398
Primary graft dysfunction, n (%)	21 (10.8)	22 (16.9)	0.112

GV, graft volume; HA, hepatic artery; LDLT, living-donor liver transplantation; MELD, model for end-stage liver disease; PV, portal vein; SLV, standard liver volume.

and 41.5 (8.5), respectively. Splenectomy was performed in 165 recipients (50.9%). The mean (SD) operation time was 807 (185) min, and the mean (SD) blood loss was 7.7 (16.1) L.

Factors associated with the presence of major spontaneous portosystemic shunt vessels were evaluated (Table 1). Patients with major shunt vessels more frequently had PV thrombosis before transplantation compared with patients without major shunt vessels (27.7% vs. 4.1%, P<0.001) before transplantation. Patients with major portosystemic shunt vessels also had lower PV pressure at laparotomy (mean [SD], 23.8 [5.4] mm Hg vs. 25.0 [5.8] mm Hg; P=0.048), were more often classified as Child-Pugh class C (71.5% vs. 58.2%, P=0.015) and were more likely to receive right-side grafts, including right-lobe and posterior segment grafts (49.3% vs. 32.5%, P=0.002). There were no other differences in preoperative and operative factors between patients with and without major portosystemic shunt vessels. Although the incidence of hepatic artery thrombosis was higher in patients with major portosystemic shunts before LDLT (2.3% vs. 0.0%, P=0.033), there were no differences in other postoperative factors.

Types of Shunt Vessels

The types of major portosystemic shunt vessels (n=130; Table 2) included splenorenal shunts (n=60, 46.2%), gastroesophageal shunts (n=35, 26.9%), mesocaval shunts (n=18, 13.8%), paraumbilical shunts (n=16, 12.3%), and cavernous transformation in the hepatoduodenal ligament (n=1, 0.8%). A total of 36 patients (27.7%) had PV thrombosis, including an atrophic PV (n=3), or complete (n=14), partial (n=15), or luminal PV thrombosis (n=4). In four patients, a splenorenal shunt was used for renoportal anastomosis to establish PV inflow (Table 2).

Ligation of the Shunt Vessels and PV Pressure

Ligation of major portosystemic shunt vessels significantly increased mean (SD) PV pressure from 16.8 (3.9) mm Hg to 18.6 (4.3) mm Hg (P<0.001) and PV flow from 1.35 (0.67) mm Hg to 1.67 (0.67) mm Hg (P<0.001). Concomitant splenectomy decreased mean (SD) PV pressure by 3.9 (0.8) mm Hg.

PV Reconstruction in Patients with PV Thrombosis

For patients with PV thrombosis, graft PV inflow was established by renoportal anastomosis (n=4), interposing an internal jugular (IJ) vein graft (n=3) between the superior mesenteric vein and graft PV, thrombectomy (n=25), or direct anastomosis (n=4). The other 94 patients (72.3%) did not have PV thrombosis before LDLT.

For patients with a splenorenal shunt and severe PV thrombosis, including an atrophic PV (n=4), renoportal anastomosis was performed to establish PV inflow. Right-lobe grafts were transplanted for appropriate vascular alignment and to accommodate the vast inflow from the mesenteric, splenic, and left renal veins (Table 2).

For patients with a mesocaval shunt and severe PV thrombosis, including patients with an atrophic PV (n=2), we used IJ jump grafts. In one patient with an atrophic PV, the atrophied PV was dissected down to the junction of the mesenteric and splenic veins, and the IJ vein graft was directly anastomosed onto the exposed junction. In the other

TABLE 2. The types of the shunts and portal vein thrombosis

Shunts	PV Thrombosis	Procedures for PV Thrombosis and Major Shunts
Splenorenal shunt (n=60)	Atrophic PV (n=2)	Renoportal anastomosis using IJ vein (n=2)
	Complete (n=7)	Renoportal anastomosis using IJ vein (n=2)
		Thrombectomy+shunt ligation (n=5)
	Partial (n=6)	Thrombectomy+shunt ligation (n=6)
	Luminal (n=1)	Direct anastomosis+shunt ligation (n=1)
	No PV thrombosis (n=44)	Shunt ligation (n=36)
		No (n=7) or incomplete (n=1) shunt ligation, followed by secondary ligation (n=4)
Gastroesophageal shunt (n=35)	Complete (n=5)	Thrombectomy+shunt ligation (n=5)
	Partial (n=3)	Thrombectomy+shunt ligation (n=3)
	Luminal (n=2)	Direct anastomosis+shunt ligation (n=2)
	No PV thrombosis (n=25)	Shunt ligation (n=21)
		No shunt ligation (n=4), followed by secondary ligation (n=3)
Mesocaval shunt (n=18)	Atrophic PV (n=1)	Interposition using IJ vein+shunt ligation (n=1)
	Complete (n=1)	Interposition using IJ vein (behind pancreas)+shunt ligation (n=1)
	Partial (n=3)	Thrombectomy+shunt ligation (n=2)
		Thrombectomy+incomplete shunt ligation, followed by secondary ligation (n=1)
	No PV thrombosis (n=13)	Shunt ligation (n=13)
Paraumbilical shunt (n=16)	Partial (n=3)	Thrombectomy+shunt ligation (n=3)
	Luminal (n=1)	Direct anastomosis+shunt ligation (n=1)
	No PV thrombosis (n=12)	Shunt ligation (n=12)
Cavernous transformation (n=1)	Complete (n=1)	Interposition using IJ vein (behind pancreas)

IJ, internal jugular; PV, portal vein.

patient with complete PV thrombosis and a very fragile PV wall caused by cholangitis, the IJ vein graft was anastomosed to the mesenteric vein in an end-to-side fashion, tunneled behind the pancreas neck and connected to the graft's PV.

For the patient with cavernous transformation, the shunt vessels in the hepatoduodenal ligament were divided under mechanical portocaval shunting from the inferior mesenteric vein into the axillar vein. The IJ vein graft was connected to the mesenteric vein in an end-to-end fashion, tunneled behind the pancreas neck, and was connected to the graft's PV.

Untied or Newly Created Shunt Vessels

Ligation of the major shunt vessels was not performed in 13/130 patients (10.0%), and a new hemiportocaval shunt was created in another patient. Therefore, 14 patients had major shunt vessels after LDLT. The reasons for having patent major shunt vessels after LDLT included undetected vessels (n=9), incomplete ligation (n=2), or the shunt was newly created or left open to maintain high PV pressure after reperfusion (n=3). Nine patients (62.3%) required secondary interventions (Table 3, Fig. 1). Among them, six cases had small-for-size graft syndrome like primary graft dysfunction, and one had cholangitis caused by biliary anastomotic stricture after LDLT.

PV flow was significantly lower in the patients who underwent secondary ligation of the major shunt vessels (n=9) than in the patients without the secondary procedure (n=121) (mean [SD], 0.96 [0.25] L/min vs. 1.62 [0.62] L/min; P=0.007). By contrast, PV pressure at the end of surgery was not significantly different between these two groups of patients (18.6 [3.9] mm Hg vs. 17.1 [4.4] mm Hg, P=0.604).

Graft Survival

The presence of major shunt vessels or PV thrombosis did not significantly affect graft survival. The 1- and 5-year cumulative graft survival rates were 90.7% and 83.0%, respectively, in patients without major shunts vessels versus 86.1% and 77.2%, respectively, in patients with major shunt vessels (P=0.195). The 1- and 5-year cumulative graft survival rate was 97.8% and 82.3%, respectively, in patients without PV thrombosis versus 84.0% and 70.6%, respectively, in patients with PV thrombosis (P=0.119).

DISCUSSION

In deceased-donor whole-liver transplantation, it is generally considered that special interventions are not necessary for spontaneous portosystemic shunts or hypersplenism. In Western countries in particular, nonsurgical transjugular intrahepatic portosystemic shunts have supplanted surgical shunts for pretransplantation management of portal hypertension and achieved sufficient portal decompression (4–6). In LDLT, however, there is no consensus on whether spontaneous portosystemic shunts should be obstructed, although some reports have described secondary interventions for patent portosystemic shunts with portal steal phenomenon (13–15). Moreover, the beneficial effects of surgically created portocaval shunts for small-for-size grafts have been widely advocated in recent years (16, 17). Nevertheless, there is no consensus on whether the shunt should be closed, kept, or

TABLE 3. The patients who underwent secondary intervention for obstructing shunt vessels after LDLT

Case No.	Age, Sex	Graft	GV/SLV ratio (%)	Shunt Type	Reason for Left Open	PV Pressure (mm Hg)	PV Flow (mL/min)
1	40, M	Left	28.9	Splenorenal	Unrecognized shunts	N/A	1150
2	47, F	Left	40.5	Splenorenal	Unrecognized shunts	N/A	770
3	53, F	Left	38.2	Splenorenal	Unrecognized shunts	22	1500
4	40, M	Left	44.7	Mesocaval	Incomplete shunt ligation	15	980
5	53, M	Right	42.9	Gastroesophageal	Unrecognized shunts	12	900
6	51, F	Post	38.6	Splenorenal	Unrecognized shunts	15	790
7	47, F	Left	23.7	Hemiportocaval	Created for high PV pressure	21	270
8	47, F	Left	35.6	Gastroesophageal	Left open for high PV pressure	21	1340
9	62, F	Left	35.4	Gastroesophageal	Left open for high PV pressure	24	990

Case No.	Intervention After LDLT	Indication	Method	Outcome
1	1st day	Decreased PV flow Graft dysfunction	Relaparotomy	Treated
2	133th day	Risky gastric varices	BRTO	Treated
3	82th day	Risky gastric varices	BRTO	Treated
4	1st day	Decreased PV flow Graft dysfunction	Relaparotomy	Treated
5	8th day	Decreased PV flow Graft dysfunction	Relaparotomy	Treated
6	22th day	Decreased PV flow Graft dysfunction	BRTO	Dead
7	4th day	Decreased PV flow Graft dysfunction	Relaparotomy	Treated
8	57th day	Encephalopathy	Relaparotomy	Treated
9	8th day	Decreased PV flow Graft dysfunction	Relaparotomy	Dead

BRTO, balloon-occluded retrograde transvenous obliteration; GV, graft volume; LDLT, living-donor liver transplantation; N/A, not applicable; PV, portal vein; SLV, standard liver volume.
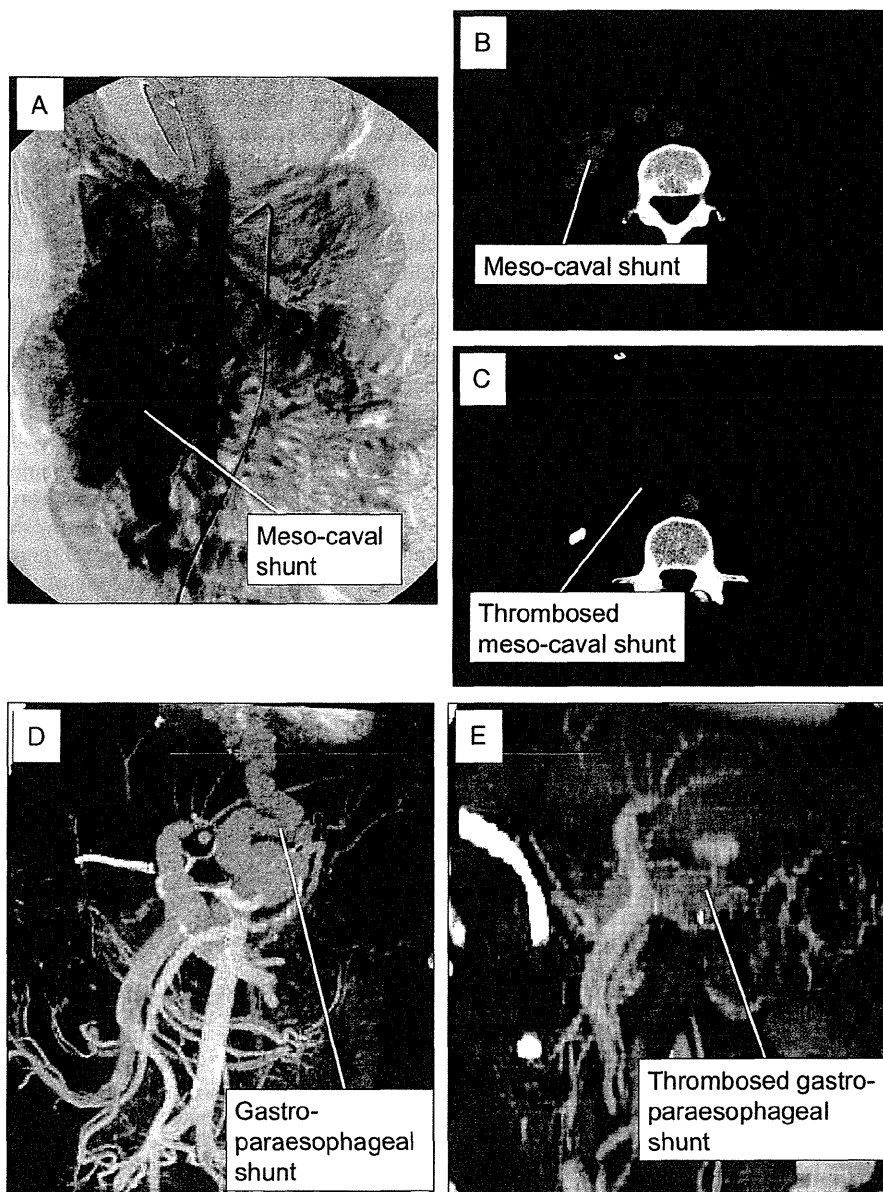
FIGURE 1. The cases of patient major shunt vessels requiring secondary intervention: Case 4 (A–C) and Case 8 (C, D). Mesenteric arterioportogram (A) and computed tomographic scan (B) showed portal steal caused by patent major mesocaval shunt, followed by surgical ligation (C). Multidetector computed tomographic image of patent gastroesophageal shunt after LDLT (D), followed by surgical ligation (E).

created, nor have the indications, such as PV pressure of PV flow, for shunt management been assessed.

In our institute, the management of portal hemodynamic status has changed considerably with our accumulating experience. Before 2000, we did not perform shunt ligation or splenectomy. However, since 2000, when we experienced a case of graft dysfunction caused by portal steal through a splenorenal shunt, we have ligated the major shunts, whenever possible. In 2001, we started to apply splenic artery ligation for patients with small-for-size graft dysfunction and increased PV pressure and then adopted splenectomy in 2005 (*18, 19*).

Following several reports published in the mid-2000s showing the beneficial effects of creating portocaval shunt for reducing PV pressure and PV flow, we created portocaval shunts or kept the major shunts in three patients to reduce high PV pressure after reperfusion, albeit with poor outcomes (*20*). These three cases showed more graft portal resistance caused by dynamic graft regeneration and reduced PV flow, which was diverted into the portosystemic shunts (*10, 12, 15*). Hemiportocaval shunting is considered to be neither stable nor safe because the flow rate into the graft and shunt cannot be controlled in a dynamically regenerating liver graft (*20*). In fact, a

similar discussion was previously reported in the context of portal steal phenomenon in auxiliary partial liver transplantation, and a consensus was obtained for ligating the PV of the native liver to provide constant PV flow into a regenerating auxiliary graft (21, 22). Thus, our current strategy for the management of PV hemodynamic status in LDLT (i.e., shunt ligation to prevent portal stealing and splenectomy for PV decompression) simplifies and normalizes PV hemodynamic management.

We have implemented several technical refinements to approach and treat portosystemic shunts, including en bloc stapling division of gastroesophageal varices and a direct approach for splenorenal shunts. Gastroesophageal shunts are often coiled or tortuous, engorged with a thin wall, sometimes multiple in number, and are usually buried in the retroperitoneum on the diaphragmatic crus (15, 23). Because manual isolation and ligation of such vessels is technically very difficult, our technique to divide these vessels, including the left gastric artery en bloc, is safe and simultaneously decreases portal inflow through the left gastric artery (23).

The approach for splenorenal shunts is also technically demanding. Lee et al. (24) recently reported a novel technique involving ligation of the left renal vein to prevent portal stealing through the splenorenal shunt. However, they also reported that ligation of the left renal vein decreased kidney size in 75% of the recipients. Therefore, they concluded that the procedure should be limited to a life-saving procedure (24). We expose the left renal vein and follow it to identify splenorenal shunts originating from the left adrenal vein. We think that normal anatomic structures, including the left renal vein and left adrenal vein, have appropriate venous shapes and thicknesses, unlike abnormal venous shunts, and following such veins can be performed safely.

The surgical technique to establish PV inflow is another issue that needs to be addressed for patients with portosystemic shunts. We use corkscrew technique for PVs extending into the splenomesenteric junction. For atrophic PV, we consider patch plasty, renoportal anastomosis, or placing an interposition graft under the pancreas neck between the superior mesenteric vein and the graft's PV. Renoportal anastomosis may be applied for patients with a splenorenal shunt (25). To place an interposition graft, it is not always possible to procure a long venous segment to join the superior mesenteric vein with the graft PV over the pancreas, especially in Japan, where deceased-donor venous grafts are rare (26). Instead, we use the IJ vein, which is tunneled under the pancreas neck. Nevertheless, it is necessary that sufficient PV inflow is maintained after obstructing the major shunts. Indeed, we recently reported that a postreperfusion PV flow of less than 1 L/min is a significant risk factor for relaparotomy for inadequate PV flow (27).

Pretransplantation evaluation of PV hemodynamic status is useful to identify the major shunt to be ligated. To achieve this, we have used multidetector-row computed tomography (MDCT) to provide three-dimensional images of PV circulation since 2007. Numerous reports have confirmed the usefulness of MDCT for visualizing the arterial, portal, and venous vasculature systems (15). Although six patients before 2006 had undetected or incompletely ligated shunts requiring secondary intervention, there have been no further cases after the introduction of three-dimensional MDCT. If PV flow after

reperfusion was less than 1 L/min, cineportograms could be performed, as suggested by Moon et al. (15).

PV hemodynamics is influenced by various factors including graft inflows and outflows, graft compliance, and central venous pressure. Partial LDLT grafts are more susceptible to these changes than the whole-liver graft (28). In the nine cases undergoing secondary intervention for PV stealing phenomenon, six had primary graft dysfunction (29), and one had cholangitis caused by biliary anastomotic stricture after LDLT. Moreover, graft regeneration itself causes decreased graft compliance, and all the partial regenerating grafts have such risks as portal stealing during regeneration (28). Such events are difficult to be forecasted, and because PV stealing with insufficient graft perfusion causes secondary graft injuries, we believe that major portosystemic shunts should be obstructed during transplantation.

Our principle in managing PV hemodynamics in LDLT is represented by simplification and normalization. By obstructing the abnormal portosystemic shunts, all the mesenteric PV flow runs into the LDLT graft without stealing, although PV pressure increases. We obstruct major (defined as ≥10 mm in size on preoperative MDCT) shunts after reperfusion. Thereafter, splenectomy is performed if PV pressure after shunt ligation is 20 mm Hg or greater for PV decompression. Although both procedures seem opposite, they are common in treating abnormal PV hemodynamics caused by end-stage liver diseases. The combination of both procedures simplify and normalize PV hemodynamics and is in contrast to preserved major portosystemic shunts without splenectomy resulting in keeping hyperdynamic PV flow with stealing.

In conclusion, it is an appropriate option to obstruct the major portosystemic shunt vessels to ensure adequate graft inflow in LDLT.

MATERIALS AND METHODS

Patients

Between May 1997 and June 2012, 381 adult-to-adult LDLTs were performed at Kyushu University Hospital, under the approval from the Ethics and Indications Committee of Kyushu University. Cases of acute liver failure (n=56) and LDLT using dual grafts (n=1) were excluded from the present analyses. Thus, 324 adult-to-adult LDLTs for chronic hepatic disorders were included in the current analyses. A total of 130 patients had major spontaneous portosystemic shunts (diameter, ≥10 mm on computed tomography) before LDLT, and 194 patients did not. The mean (SD) follow-up time was 4.8 (3.6) years.

Graft Selection

Grafts were selected as previously described (30). Left-lobe grafts were used as the primary graft type if the desired GV/SLV ratio was 35% or greater. Right-lobe grafts were used if the simulated GV/SLV ratio of the left-lobe graft was less than 35% and the donor's remnant liver volume was 35% or greater. Posterior segment grafts were used if GV/SLV ratio of the posterior segment graft was 35% or greater with isolated branching of the posterior PV from the main PV and if both left and right-lobe grafts were not available.

Transplant Procedures

Donor parenchymal transection was performed using the Cavitron Ultrasonic Surgical Aspirator (Valleylab Inc., Boulder, CO) with the hanging maneuver (31). After donor hepatectomy, the graft was perfused, weighed, and stored in University of Wisconsin solution (Viaspan; DuPont Inc., Wilmington, DE).

After recipient hepatectomy, the grafts were transplanted in a piggyback fashion. The orifice of the recipient's hepatic vein was enlarged with an incision

on the vena cava for the venous anastomosis to provide sufficient outflow. After venous anastomoses, the PV was reconstructed and reperfused. Subsequent arterial reconstruction was performed under a microscope. If indicated, splenectomy was performed as previously described (*31*). Biliary reconstruction was performed by duct-to-duct biliary anastomosis whenever possible.

Ligation or Division of the Major Shunt Vessels

Since 2000, we have ligated all of the identified major (≥10 mm) portosystemic shunt vessels during LDLT, whenever indicated. The presence of such major portosystemic shunts was diagnosed using MDCT after operation. The shunts are controlled and left open during the anhepatic phase to minimize portal venous congestion and are ligated after reperfusion.

To control splenorenal or gastrorenal shunts, intraoperative sonography was used to identify the left renal vein in the retroperitoneum near the left side of the inferior mesenteric vein. The transverse mesocolon was retracted in a cephalad direction to provide an adequate surgical field. The retroperitoneum was opened, and the left renal vein was identified. By following the left renal vein, a dilated splenorenal shunt was identified on the cranial side and was then controlled as appropriate.

For gastroesophageal shunts, the dilated coronary vein was carefully dissected from the retroperitoneum and controlled, followed by its ligation, before May 2011. However, because this is a technically difficult procedure, caused by the tortuously dilated coronary veins with minor collateral vessels, we have since applied endostapling devices to the base of the left gastric ligament, including the left gastric artery, engorged coronary vein, and collateral vessels, followed by en bloc division using endostapling devices (Echelon Flex Endopath TM Staplers 60-2.5; Ethicon Endo-Surgery Inc., Cincinnati, OH) and mass suturing with continuous 3-0 Prolene sutures with an SH needle (Ethicon Inc., Somerville, NJ) (*23*).

Mesocaval shunts were identified in the retroperitoneum on a case-by-case basis. We routinely ligate the major inflow into the mesocaval shunts and the major outflow into the vena cava.

Establishment of PV Inflow

The presence of major shunt vessels might indicate PV thrombosis or atrophy. Eversion or corkscrew procedures were performed for PV thrombectomy (*32*). Renoportal anastomosis was indicated for complete PV thrombosis with a fragile or atrophic PV vein wall with numerous splenorenal shunts. The left renal vein was controlled after mobilization of the duodenum. End-to-end PV reconstruction was performed using an IJ vein graft with continuous 6-0 polydiaxanone sutures.

For an atrophied PV or complete PV thrombosis with a fragile PV wall, without splenorenal shunts, PV reconstruction was performed using IJ jump grafts, which were connected to the mesenteric-splenic junction or the mesenteric vein. The IJ graft was then tunneled behind the pancreas neck to connect to the PV.

Splenectomy

The indications for splenectomy during LDLT include hypersplenism, PV pressure of 20 mm Hg or greater, and patients with hepatitis C treated with interferon after LDLT. We have introduced tieless splenectomy (*19*) using a vessel-sealing system (LigaSure Atlas; Valleylab Inc., Boulder, CO) and endostapling devices (Echelon Staplers 60-2.5; Ethicon Endo-Surgery Inc.).

Measurement of Portal Hemodynamic Properties

PV pressure was continuously monitored during surgery using a cannula (Medicut LCV-UK catheter 14 GTM; Nippon Sherwood Inc., Tokyo, Japan) placed in the superior mesenteric vein through a terminal jejunal vein. Intraoperative PV flow (L/min) was measured in the recipients using an ultrasonic transit time flow meter (Transonic System, Ithaca, NY) after establishing hepatic artery flow and reperfusion.

Posttransplantation Medical Care

The basic immunosuppression protocol consisted of tacrolimus or cyclosporine with mycophenolate mofetil and steroids. The target tacrolimus level was 10 to 14 ng/mL at 1 month after LDLT and was decreased to 7 to 10 ng/mL during the next few months. The target cyclosporine level was 150 to 250 ng/mL at 1 month after LDLT and was decreased to 100 to 150 ng/mL during the next few months.

Primary graft dysfunction was defined as graft insufficiency with possible early graft loss, without technical, anatomic, immunologic, or hepatitis-related issues. Primary graft dysfunction was detected as delayed hyperbilirubinemia, with a total bilirubin of 20 mg/dL or greater, usually occurring 7 days after surgery and persisting for 7 or more consecutive days. It was treated by plasma exchange (*29*).

Statistical Analysis

All analyses were conducted in a retrospective manner. Values are expressed as the mean (SD). Variables were analyzed using chi-square tests for categorical values or the Mann-Whitney test for continuous variables. Cumulative survival was determined using the Kaplan-Meier method with log-rank tests. $P<0.05$ was considered statistically significant.

REFERENCES

1. Collini FJ, Brener B. Portal hypertension. *Surg Gynecol Obstet* 1990; 170: 177.
2. Rössle M, Siegerstetter V, Huber M, et al. The first decade of the transjugular intrahepatic portosystemic shunt (TIPS): state of the art. *Liver* 1998; 18: 73.
3. Cosenza CA, Hoffman AL, Friedman ML, et al. Transjugular intrahepatic portosystemic shunt: efficacy for the treatment of portal hypertension and impact on liver transplantation. *Am Surg* 1996; 62: 835.
4. Narahara Y, Kanazawa H, Kawamata H, et al. A randomized clinical trial comparing transjugular intrahepatic portosystemic shunt with endoscopic sclerotherapy in the long-term management of patients with cirrhosis after recent variceal hemorrhage. *Hepatol Res* 2001; 21: 189.
5. Tomikawa M, Hashizume M, Okita K, et al. Endoscopic injection sclerotherapy in the management of 2105 patients with esophageal varices. *Surgery* 2002; 131: S171.
6. Yanaga K, Tzakis AG, Shimada M, et al. Reversal of hypersplenism following orthotopic liver transplantation. *Ann Surg* 1989; 210: 180.
7. Hadengue A, Lebrec D, Moreau R, et al. Persistence of systemic and splanchnic hyperkinetic circulation in liver transplant patients. *Hepatology* 1993; 17: 175.
8. Piscaglia F, Zironi G, Gaiani S, et al. Systemic and splanchnic hemodynamic changes after liver transplantation for cirrhosis: a long-term prospective study. *Hepatology* 1999; 30: 58.
9. Jiang SM, Zhang QS, Zhou GW, et al. Differences in portal hemodynamics between whole liver transplantation and living donor liver transplantation. *Liver Transpl* 2010; 16: 1236.
10. Jang YJ, Kim KW, Jeong WK, et al. Influence of preoperative portal hypertension and graft size on portal blood flow velocity in recipient after living donor liver transplantation with right-lobe graft. *AJR Am J Roentgenol* 2010; 194: W165.
11. Sugimoto H, Kato K, Hirota M, et al. Serial measurement of Doppler hepatic hemodynamic parameters for the diagnosis of acute rejection after live donor liver transplantation. *Liver Transpl* 2009; 15: 1119.
12. Nakanishi S, Shiraki K, Yamamoto K, et al. Early graft hemodynamics in living related liver transplantation evaluated by Doppler ultrasonography. *Int J Mol Med* 2004; 14: 265.
13. Kita Y, Harihara Y, Sano K, et al. Reversible hepatofugal portal flow after liver transplantation using a small-for-size graft from a living donor. *Transpl Int* 2001; 14: 217.
14. Sekido H, Matsuo K, Takeda K, et al. Severe fatty change of the graft liver caused by a portosystemic shunt of mesenteric varices. *Transpl Int* 2002; 15: 259.
15. Moon DB, Lee SG, Ahn C, et al. Application of intraoperative cine-portogram to detect spontaneous portosystemic collaterals missed by intraoperative Doppler exam in adult living donor liver transplantation. *Liver Transpl* 2007; 13: 1279.
16. Troisi R, Ricciardi S, Smeets P, et al. Effects of hemi-portocaval shunts for inflow modulation on the outcome of small-for-size grafts in living donor liver transplantation. *Am J Transplant* 2005; 5: 1397.
17. Yamada T, Tanaka K, Uryuhara K, et al. Selective hemi-portocaval shunt based on portal vein pressure for small-for-size graft in adult living donor liver transplantation. *Am J Transplant* 2008; 8: 847.